Subband structure of a two-dimensional electron gas formed at the polar surface of the strong spin-orbit perovskite KTaO₃

P. D. C. King,[1] R. H. He,[2] T. Eknapakul,[3] S.-K. Mo,[2] Y. Kaneko,[4] S. Harashima,[5] Y. Hikita,[6,7] M. S. Bahramy,[8] C. Bell,[6,7] Z. Hussain,[2] Y. Tokura,[4,8,5] Z.-X. Shen,[6,7] H. Y. Hwang,[6,7,8] F. Baumberger,[1,*] and W. Meevasana[3,9,†]

[1]*School of Physics and Astronomy, University of St. Andrews, St. Andrews, Fife KY16 9SS, United Kingdom*
[2]*Advanced Light Source, Lawrence Berkeley National Lab, Berkeley, CA 94720, USA*
[3]*School of Physics, Suranaree University of Technology and Synchrotron Light Research Institute, Nakhon Ratchasima, 30000, Thailand*
[4]*Multiferroics Project, ERATO, JST, Tokyo 113-8656, Japan*
[5]*Department of Applied Physics, University of Tokyo, Bunkyo-ku, Tokyo 113-8656, Japan*
[6]*Departments of Physics and Applied Physics, Stanford University, CA 94305, USA*
[7]*SIMES, SLAC National Accelerator Laboratory, 2575 Sand Hill Road, CA 94025, USA*
[8]*Correlated Electron Research Group (CERG), RIKEN-ASI, Wako 351-0918, Japan*
[9]*Thailand Center of Excellence in Physics, CHE, Bangkok, 10400, Thailand*
(Dated: August 11, 2011)

We demonstrate the formation of a two-dimensional electron gas (2DEG) at the (100) surface of the $5d$ transition-metal oxide KTaO₃. From angle-resolved photoemission, we find that quantum confinement lifts the orbital degeneracy of the bulk band structure and leads to a 2DEG composed of ladders of subband states of both light and heavy carriers. Despite the strong spin-orbit coupling, we find no experimental signatures of a Rashba spin splitting, which has important implications for the interpretation of transport measurements in both KTaO₃- and SrTiO₃-based 2DEGs. The polar nature of the KTaO₃(100) surface appears to help mediate formation of the 2DEG as compared to non-polar SrTiO₃(100).

PACS numbers: 73.21.Fg,73.20.-r,79.60.Bm

Today's electronic devices largely rely on control of the conductivity of two-dimensional (2D) electron channels in semiconductor hosts. Creating such 2D electron gases (2DEGs) in oxides, which in bulk form generally show much larger and more diverse responses to external stimuli, holds the potential for devices with functionalities well beyond what we have experienced to date [1]. The prototypical example of an oxide 2DEG, formed when SrTiO₃ is interfaced to the polar surface of another perovskite oxide [2], has indeed proved a very rich system [3, 4]. Recently, it was discovered that oxygen vacancies could mediate formation of a similar 2DEG at the bare surface of SrTiO₃ [5, 6], providing an exciting opportunity for the realization of 2DEGs in more exotic parent materials than has been achieved via interface engineering.

Of particular interest are $5d$ transition metal oxides (TMOs), whose large spin-orbit interactions offer the potential to incorporate the spintronic functionality sought in emerging schemes of semiconductor electronics [7–9] into all-oxide devices. Despite the extended nature of $5d$ atomic orbitals, the interplay of their large spin-orbit interactions with even a modest Coulomb repulsion yields pronounced signatures of electron correlations in these materials, such as the formation of Mott insulating states [10–12] and possible correlated topological insulators [13, 14], suggesting $5d$ TMOs could provide a novel and potentially very rich host for engineering of artificial 2D electron systems. Understanding the interplay of strong spin-orbit coupling, quantum confinement, and

correlations within such a 2DEG is an essential step towards realizing their potential for practical applications. To date, this has been hampered by the difficulty of generating 2DEGs in $5d$ oxides via interface engineering.

Here, we show that a 2DEG can be created at the (100) surface of the $5d$ perovskite KTaO₃. Exploiting its surface-localized nature, we utilize angle-resolved photoemission (ARPES) to provide the first direct measurement of the subband structure of a $5d$-oxide 2DEG. Our measurements, supported by model calculations, reveal an important role of multi-orbital physics in this system. Surprisingly, however, they do not show any significant Rashba spin-splitting of the 2DEG, which might naturally be expected.

Single-crystal undoped KTaO₃ (commercial samples from Crystal Base Jpn.) and lightly electron-doped $K_{1-x}Ba_xTaO_3$ (flux-grown samples, $x < 0.001$) was measured. The Ba-doping yields a small residual bulk conductivity ($n \sim 1 \times 10^{19}$ cm^{-3} from Hall effect measurements) which eliminates charging effects in ARPES, but does not otherwise affect the conclusions of this work. ARPES measurements ($T = 20$ K, $h\nu = 45-85$ eV) were performed using a Scienta R4000 hemispherical analyzer at beamline 10.0.1 of the Advanced Light Source with an energy resolution between 8 and 35 meV, and an angular resolution of 0.35°. Multiple samples were cleaved along the (100) surface at the measurement temperature in a pressure better than 3×10^{-11} mbar.

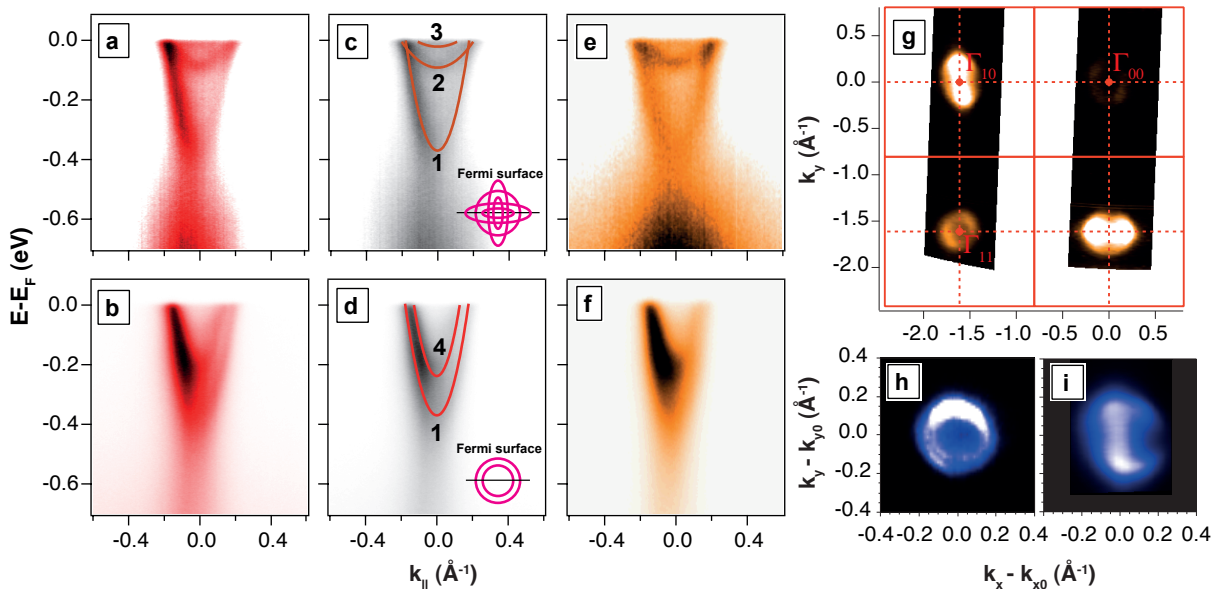For the insulating samples investigated here, no bulk bands would be expected in the vicinity of the Fermi

FIG. 1: ARPES measurements, recorded following exposure to intense UV synchrotron light, of the dispersion of surface 2DEG states along the Γ–X direction of (a–d) lightly bulk-doped and (e–f) undoped $KTaO_3$, measured using a photon energy of 55 eV. Measurements were performed using (a,c,e) s-polarized and (b,d,f) p-polarized light in the Γ_{10} and Γ_{11} Brillouin zones, respectively. In (c,d) a schematic band topology is superimposed on the data reproduced from panels (a,b). (g) Fermi surface topology covering multiple Brillouin zones, measured using a photon energy of 85 eV and p-polarized light. Detailed Fermi surface maps around the (h) Γ_{11} and (i) Γ_{10} points ($h\nu = 55$ eV) using p- and s-polarized light, respectively.

level. In contrast, our surface-sensitive ARPES measurements (Fig. 1) reveal a complex electronic structure with at least 4 dispersive electron-like bands which cross the Fermi level (Fig. 1a–f). This directly indicates that the surface of this material has become strongly conducting, in contrast to its bulk. The same bands are observed here for both lightly bulk-doped (Fig. 1(a,b)) and insulating undoped (Fig. 1(e,f)) $KTaO_3$ samples, ruling out bulk states as the source of the measured bands. Additionally, photon-energy-dependent measurements (not shown) reveal that these states have no dispersion along k_z. They are therefore two-dimensional electronic states confined near the surface, unlike the three-dimensional bulk states.

After cleaving the sample, and upon exposure to intense UV light, the Fermi wavevectors of the states increase (Fig. 2(a)) and then saturate to give the electronic structure shown in Fig. 1. At the same time, the O $2p$ valence bands shift to higher binding energy (Fig. 2(b)), indicating a downward bending of the electronic bands relative to the Fermi level in the vicinity of the surface. This causes a build-up of electronic charge near to the surface [15]. In conventional semiconductors, these electrons do not occupy the original bulk electronic states: the electrostatic band bending potential, together with the potential step at the surface itself, forms a quantum well which causes the conduction bands to reconstruct into ladders of partially-filled two-dimensional subbands

in the vicinity of the surface [16]. The two-dimensional metallic states that we measure here by ARPES are a direct observation of such quantum-confined states in a $5d$ TMO. Together with the shift of the valence band, these measurements present unambiguous evidence for formation of a conducting 2DEG at the bare surface of $KTaO_3$. This formation of the 2DEG is accompanied by the emergence of an in-gap defect peak, indicative of oxygen vacancies at the surface (Fig. 2(a)). This suggests that the 2DEG is formed to screen the positive charge resulting from a UV-stimulated desorption of oxygen from the surface plane, and this provides the microscopic mechanism driving the surface-localized insulator-to-metal transition, as recently suggested for a surface 2DEG created in $SrTiO_3$ [5].

The rate of formation of the 2DEG states with irradiation dose is, however, more rapid than for $SrTiO_3$, as shown in Fig. 2(a). We speculate that this could be due to the polar nature of the $KTaO_3$ surface (Fig. 2(c)), which may lower the formation energy for oxygen vacancies in order to compensate the polarization discontinuity at the surface. From a comparison of model calculations (discussed below) to the ARPES measurements, we estimate the density of the 2DEG to be $N \approx 2 \times 10^{14}$ cm^{-2}, which is slightly lower than, but approaching, the $0.5e^-$ per unit cell (3.3×10^{14} cm^{-2}) which would be expected from a simple polar catastrophe argument. Thus, while an interface between a polar and non-polar sur-
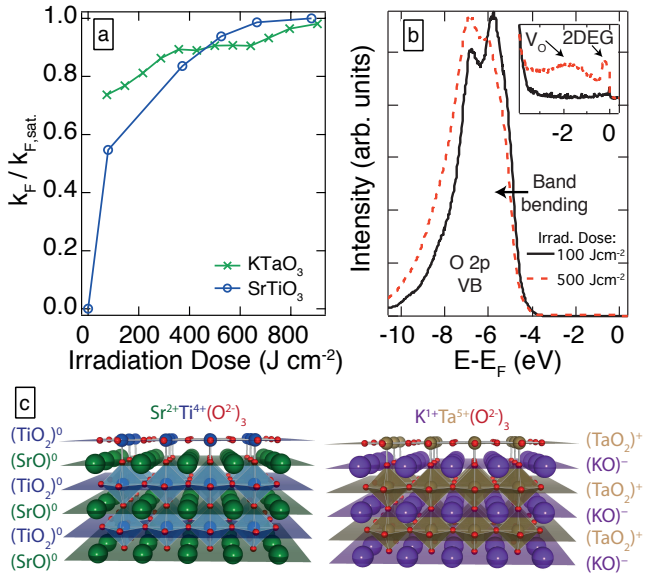
FIG. 2: (a) Irradiation dose-dependence of Fermi wavevector of the deepest d_{xy}-type band of the surface 2DEG formed in SrTiO$_3$ and KTaO$_3$ upon exposure to intense UV light, normalized to its saturation value. (b) O 2p valence bands of KTaO$_3$ after small and heavier irradiation dose, with the near-E_F emission magnified in the inset. (c) Structure of SrTiO$_3$ and KTaO$_3$, composed of alternating neutral or positively and negatively charged planes, respectively.

face does not always appear necessary to create an oxide 2DEG [5, 6], these measurements suggest that it may help mediate its formation, either via intrinsic electronic reconstruction [17] or by promoting the formation of extrinsic defects.

Bands 1 and 4 of the resulting 2DEG (Fig. 1d) have a light effective mass of ~ 0.3 m$_e$, obtained from parabolic fits to their measured dispersion. This is almost a factor of 2 smaller than recently determined for a surface 2DEG in SrTiO$_3$ [5], suggesting that KTaO$_3$ could provide a superior platform to its workhorse counterpart of SrTiO$_3$ in which to develop high-mobility oxide electronics. We also observe a tail of intensity below the band bottom of these states, characteristic of the spectral function in strongly-interacting systems. This hints at an important role of electron correlations in this system, signifying a liquid-like state as was recently inferred for 2DEGs at SrTiO$_3$ surfaces and interfaces [5, 18]. Thus, KTaO$_3$-based 2DEGs may provide an appealing route to combine the exotic phase diagrams that often accompany strong electron correlations with a system which supports very mobile carriers, useful for device applications. In this respect, we note that a record mobility for a TMO 2DEG of 7000 cm^{2}V^{-1}s^{-1} was recently achieved in a KTaO$_3$ electric double-layer transistor [19]. The same system was also found to superconduct, a property which has not to date been obtained in the bulk of this material.

Co-existing with these mobile states, we additionally observe much heavier carriers (bands 2 and 3 in Fig. 1(c), $m^* \sim 2-3$ m$_e$). Together, bands 1–4 contribute both concentric circular (Fig. 1(g,h)) as well as elliptical (Fig. 1(g,i)) electron pockets to the Fermi surface, suggesting that the electronic structure observed here is derived from multiple orbitals of different symmetries. Indeed, the bulk conduction bands of KTaO$_3$, as in SrTiO$_3$, are formed from three t_{2g} orbitals [20]. In the simplest picture, these form three d_{xy}-, d_{xz}- and d_{yz}-derived interpenetrating ellipsoids, giving rise to one heavy and two light bands along the $\langle 100 \rangle$ directions (Fig. 3(a)). However, spin-orbit coupling in KTaO$_3$ leads to a strong orbital hybridization. As shown in Fig. 3(b), this lifts the Γ-point degeneracy by splitting off a light band above a pair of light and heavy bands by a large energy gap of $\Delta_{so} \sim 400$ meV. The electronic bands we observe, however, have quite different characteristics (Fig. 1), with at least two light bands (1 and 4) located at higher binding energies than the first heavy state (band 2). We attribute this to the influence of quantum confinement, which can significantly influence the orbital occupancy.

We illustrate this first for the simpler case of a SrTiO$_3$ surface-2DEG (Fig. 3(c)), where the spin-orbit split-off energy is small and can be neglected to first approximation. We model the electronic structure using a tight-binding supercell with band bending included via additional on-site potential terms, similar to the method introduced by Stengel [21]. This model is solved self-consistently with Poisson's equation, incorporating an electric-field-dependent dielectric constant [22], to yield the electronic structure shown in Fig. 3(c).

Starting at the highest binding energies, a ladder of multiple d_{xy}-derived subbands are predicted. These are in good agreement with the multiple light states observed by ARPES (Fig. 3(c)). This orbital assignment is consistent with their circular Fermi surfaces [5] and with the ladder of isotropic states recently observed in quantum oscillation measurements of δ-doped SrTiO$_3$ quantum wells [23, 24]. Due to the small interlayer hopping between d_{xy} orbitals along the confinement direction, or equivalently their heavy effective mass along k_z, the most deeply bound of these subbands have wavefunctions which are dominantly localized on successive atomic planes below the surface, similar to first-principles calculations for a SrTiO$_3$ interfacial 2DEG [25], explaining why they can be clearly observed in the ARPES [26]. On the other hand, the $d_{xz/yz}$ orbitals have a significantly larger overlap along k_z, and so the subbands deriving from these orbitals have envelope wavefunctions which are much more extended along the confinement direction. The binding energy of the heavy and light pairs of $d_{xz/yz}$-derived subbands is correspondingly reduced [6], lifting the orbital degeneracy of the bulk band structure. This effect can be seen in our measurements, where a heavy band, whose binding energy and dispersion are in
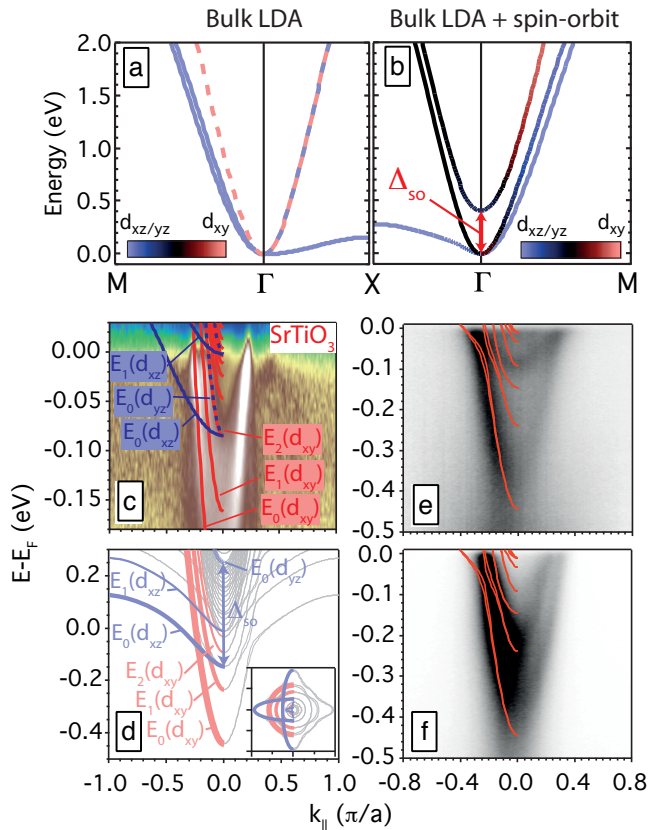
FIG. 3: LDA calculations of the bulk electronic structure and orbital character of KTaO$_3$ (a) excluding and (b) including spin-orbit coupling. (c) Comparison of measured dispersions to model tight-binding calculations of a surface 2DEG in SrTiO$_3$. (d) Equivalent calculations for a KTaO$_3$ 2DEG including spin-orbit coupling. The coloured lines give a schematic decomposition of its orbital makeup. (e,f) Comparison of the KTaO$_3$ calculations to the experimental data from Fig, 1(a,b) taken with s- or p-polarization, respectively.

good agreement with the calculated d_{xz}-derived subband, can just be resolved in the normalized spectrum shown in Fig. 3(c). Its very weak spectral weight in the ARPES measurement is a natural consequence of the extended nature of its wavefunction along k_z.

Analogous calculations for KTaO$_3$ [27], with spin-orbit coupling included, are shown in Fig. 3(d). These can be qualitatively understood starting from the same orbital makeup as in SrTiO$_3$, but with some important additional features: (1) the lighter of the original $d_{xz/yz}$-derived states is shifted above the Fermi level by the large spin-orbit split-off energy, Δ_{so}, lifting the Γ-point degeneracy of $d_{xz/yz}$ states that is present for SrTiO$_3$; (2) small hybridization gaps open up between the different subbands; and (3) the orbital character of the lighter bands becomes strongly mixed. These characteristics are fully consistent with the measured band structure shown in Fig. 3(e,f), although some of the more subtle features of

the calculations cannot be easily resolved experimentally.

The calculations also predict a small spin splitting of the 2DEG states around the hybridization gaps (Fig. 3(d–f)). This can be attributed to the Rashba effect which lifts spin degeneracy in the presence of a structural inversion asymmetry [29]. The symmetry breaking is provided here by the asymmetric potential well which confines the 2DEG. Indeed, a Rashba spin splitting has recently been attributed as the origin of weak antilocalization (WAL) in a KTaO$_3$ field-effect transistor [30]. However, the splitting predicted in the calculations is minute, over an order of magnitude smaller than recently observed for the seemingly similar system of a 2DEG in the heavy Bi-containing topological insulator Bi$_2$Se$_3$ [31]. This is consistent with our experimental data, where any spin splitting is too small to be resolved. We attribute this to the particular electronic states involved: the degenerate t_{2g} manifold of states at Γ is split into an effective $J = 3/2$ doublet at the conduction band edge and a $J = 1/2$ split-off band (Fig. 3(b)) [10]. This is analogous to the valence, rather than conduction, bands of typical III-V semiconductors such as GaAs. In such systems, the k-linear term in the Rashba spin-splitting of a 2D hole gas is forbidden due to symmetry, leaving the leading-order term as k^3 [32]. In the low-k regime applicable here, this yields a very small Rashba splitting despite the strong spin-orbit coupling and large potential gradient within the 2DEG. We note that it should be even smaller in SrTiO$_3$-based 2DEGs, where spin-orbit coupling is more than an order of magnitude smaller than for KTaO$_3$, raising the intriguing possibility that WAL in both KTaO$_3$ [30] and SrTiO$_3$-based [33, 34] 2DEGs is due to more exotic physics.

* Corresponding e-mail: fb40@st-andrews.ac.uk
† Corresponding e-mail: worawat@g.sut.ac.th
[1] H. Takagi and H. Y. Hwang, Science **327**, 1601 (2010).
[2] A. Ohtomo and H. Y. Hwang, Nature **427**, 423 (2004).
[3] J. Mannhart and D. G. Schlom, Science **327**, 1607 (2010).
[4] P. Zubko et al., Annu. Rev. Condens. Matter Phys. **2**, 141 (2011).
[5] W. Meevasana et al., Nature Mater. **10**, 114 (2011).

[6] A. F. Santander-Syro *et al.*, Nature **469**, 189 (2011).
[7] I. Zŭtić *et al.*, Rev. Mod. Phys. **76**, 323 (2004).
[8] H. C. Koo, *et al.*, *Science* **325**, 1515 (2009).
[9] S. Nadj-Perge, *et al.*, *Nature* **468**, 1084 (2010).
[10] B. J. Kim *et al.*, Phys. Rev. Lett. **101**, 076402 (2008).
[11] B. J. Kim *et al.*, Science **323**, 1329 (2009).
[12] S. J. Moon *et al.*, Phys. Rev. Lett. **101**, 226402 (2008).
[13] D. Pesin and L. Balents, Nature Phys. **6**, 376 (2010).
[14] A. Shitade *et al.*, Phys. Rev. Lett. **102**, 256403 (2009).
[15] P. D. C. King *et al.*, Phys. Rev. Lett. **101**, 116808 (2008).
[16] P. D. C. King *et al.*, Phys. Rev. Lett. **104**, 256803 (2010).
[17] N. Nakagawa *et al.*, Nature Mater. **5**, 204 (2006).
[18] M. Breitschaft *et al.*, Phys. Rev. B **81**, 153414 (2010).
[19] K. Ueno *et al.*, Nature Nano. **6**, 408 (2011).
[20] T. Neumann *et al.*, Phys. Rev. B **46**, 10623 (1992).
[21] M. Stengel, Phys. Rev. Lett. **106**, 136803 (2011).
[22] O. Copie *et al.*, Phys. Rev. Lett. **102**, 216804 (2009).
[23] Y. Kozuka *et al.*, Nature **462**, 487 (2009).
[24] M. Kim *et al.*, Phys. Rev. Lett. *in press*; arXiv:1104.3388.
[25] Z. S. Popović *et al.*, Phys. Rev. Lett. **101**, 256801 (2008).
[26] As the potential becomes shallower, the wavefunctions of the highest d_{xy} states within this ladder become much more delocalized along k_z, making it difficult to resolve these predicted states in the ARPES measurements.
[27] To describe the electric field-dependence of the dielectric constant, the experimental data of Ref. [28] was fit with the model descirbed in Ref. [22]. Slightly better agreement with the ARPES data was obtained by reducing the effective critical field from 1.9×10^6 Vm^{-1} to 1.1×10^6 Vm^{-1}, but this does not alter the generic subband structure or any other conclusions of this work.
[28] C. Ang *et al.*, Phys. Rev. B **64**, 184104 (2001).
[29] Y. A. Bychkov and E. I. Rashba, JETP Lett. **39**, 78 (1984).
[30] H. Nakamura and T. Kimura, Phys. Rev. B **80**, 121308 (2009).
[31] P. D. C. King *et al.*, Phys. Rev. Lett. *in press*; arXiv:1103.3220 (2011).
[32] R. Winkler, *Spin-orbit Coupling Effects in Two-Dimensional Electron and Hole Systems* (Springer, Berlin, 2003).
[33] A. D. Caviglia *et al.*, Phys. Rev. Lett. **104**, 126803 (2010).
[34] M. Ben Shalom *et al.*, Phys. Rev. Lett. **104**, 126802 (2010).